SCIENCE CHINA
Technological Sciences

• Article •

February 2017 Vol.60 No.2: 282–288
doi: 10.1007/s11431-016-0505-x

Vacuum degree effects on betavoltaics irradiated by ^{63}Ni with differently apparent activity densities

LIU YunPeng[1,2*], XU ZhiHeng[1], WANG Hao[1] & TANG XiaoBin[1,2]

[1]*Department of Nuclear Science and Engineering, Nanjing University of Aeronautics and Astronautics, Nanjing 210016, China;*
[2]*Jiangsu Key Laboratory of Material and Technology for Energy Conversion, Nanjing 210016, China*

Received June 30, 2016; accepted October 8, 2016; published online December 21, 2016

For many current betavoltaics, beta sources and PN junction energy conversion units are separated. The air gap between the two parts could stop part of decay beta particles, which results in inefficient performance of the betavoltaic. By employing ^{63}Ni with an apparent emission activity density of 7.26×10^{7} and 1.81×10^{8} Bq cm^{-2}, betavoltaic performance levels were calculated at a vacuum degree range of 1×10^{5} to 1×10^{-1} Pa and measured at 1.0×10^{5} and 1.0×10^{4} Pa, respectively. Results show that betavoltaic performance levels improve significantly as the vacuum degree increases. The maximum output power (P_{max}) exhibits the largest change, followed by short-circuit current (I_{sc}), open-circuit voltage (V_{oc}), and fill factor. The vacuum degree effects on I_{sc}, V_{oc}, and P_{max} of the betavoltaic with low apparent activity density ^{63}Ni are more significant than those of the betavoltaic with high apparent activity density ^{63}Ni. Moreover, the improved efficiencies of the measured performances are larger than the calculated efficiencies because of the low ratio of I_{sc} and reverse saturation current (I_0). The values of I_0, ideality factor, and shunt resistance were estimated to modify the equivalent circuit model. The calculation results based on this model are closer to the measurement results. The results of this research can provide a theoretical foundation and experimental reference for the study of vacuum degree effects on betavoltaics of the same kind.

vacuum degree, betavoltaic, apparent activity density, energy conversion unit, MCNP5

Citation: Liu Y P, Xu Z H, Wang H, et al. Vacuum degree effects on betavoltaics irradiated by ^{63}Ni with differently apparent activity densities. Sci China Tech Sci, 2017, 60: 282–288, doi: 10.1007/s11431-016-0505-x

1 Introduction

A betavoltaic consists of two parts, namely, a beta source and a PN junction energy conversion unit (ECU). Betavoltaics convert the electron hole pairs (EHPs) produced by the ionization trail of emitted beta particles form a beta source and traverse a semiconductor junction device to electricity. With long-lifetime, high-energy-density, amenability-to-miniaturization, and autonomous-power-supply, betavoltaics possess significant potential applications in deep-space exploration, military, and medical fields. As one of the power supply options in microelectromechanical systems, betavoltaics have gained worldwide attention in research and development [1].

Most of previous betavoltaics based on Si [2,3], GaAs [4,5], GaN [6–8], and 4H-SiC [9–11] employ a separate structure. This condition means the beta source and ECU are separated from each other. The beta source is placed near the front side of the ECU, and an air gap with about 0.1 to 1 mm width exists between the two parts [3,12–14]. The air gap can partially stop the decay beta particles. And this will result in the inefficient performance of the betavoltaic. Qiao et al. [11] demonstrated a 4H-SiC betavoltaic and got a nonideal output performance. One of the key limit factors is the energy loss in air gap. But ref. [11] didn't refer to how the air gap affected the betavoltaic performance. The stopping power for beta parti-

*Corresponding author (email: liuyp@nuaa.edu.cn)

cles in an air medium with different thicknesses has been discussed theoretically [15]. Wacharasindhu et al. [15] defined the external interaction loss by the radiation loss between the radioisotope source and the active region of the betavoltaic cell by interactions with media, including air. However, the influence of air on the betavoltaic performance was also not studied. Air rarefies as the vacuum degree increases. Therefore, it is necessary to study the vacuum degree effects on the performance of the betavoltaic.

In this paper, we present a theoretical method to study the effects of vacuum degree on the performance of a silicon betavoltaic based on beta source ^{63}Ni with different apparent activity densities. The *I-V* characteristics of betavoltaics at different vacuum degrees were measured and compared with those results by calculating. An equivalent circuit model was utilized to modify the calculation results. This study can serve as a reference to examine the vacuum degree effects on betavoltaics based on other semiconductor materials and beta sources. The result can also provide an appropriate vacuum degree in the vacuum packaging of the betavoltaic.

2 Materials and methods

2.1 Semiconductor and beta source

The threshold displacement energy is the minimum kinetic energy that an atom in a crystal needs to be permanently displaced from its lattice site to a defect position. The displacement energy of crystalline silicon atom is 14 to 21 eV. Based on the elastic collision mechanism, only the incident beta particles with more than 155 to 221 keV can make displacement damage in silicon. For the beta source, the energy spectrum is continuous. ^{63}Ni emits pure beta particles with the average energy of 17.13 keV and the maximum energy of 65.87 keV. These particles could hardly make displacement damage in silicon. Moreover, these particles can be shielded easily. Two ^{63}Ni sources with different apparent activity densities were employed in both calculation and experiment. Table 1 shows the specific parameters of ^{63}Ni. In view of technological maturity and cost [16], crystalline Si was utilized to fabricate the ECU. The substrate Si is phosphorus-doped with 9.3×10^{13} cm^{-3}, and the thickness is 300 μm. The crystal orientation is <111>.

2.2 Theoretical calculation

A theoretical calculation model was developed using the actual structural parameters of the silicon betavoltaic, including ^{63}Ni, air gap, and ECU. The energy deposition of beta particles in the ECU was calculated with the Monte Carlo N-Particle Transport Code Version 5 (MCNP5). The thickness values of ^{63}Ni were set to 0.095 and 0.293 μm, and the resulting apparent activity densities were 7.4×10^7 and 1.85×10^8 Bq cm^{-2}, respectively, as in the case of the experimental ^{63}Ni. The surface current tally card in MCNP5 was utilized to estimate the thickness of ^{63}Ni.

Changes in air density were employed to simulate the change in vacuum degree in the calculation. The calculation formula can be expressed as

$$\rho = \frac{PT_0}{TP_0}\rho_0, \tag{1}$$

where r is air density at an unknown vacuum degree (P) and unknown temperature (T), and r_0 is air density at a known vacuum degree (P_0) and known temperature (T_0). The air density is 1.1619×10^{-3} g cm^{-3} at 300 K and 1.01×10^5 Pa. Both calculation and measurement were conducted at 300 K. The vacuum degrees in the calculation are 1.0×10^5, 7.5×10^4, 5.0×10^4, 2.5×10^4, 1.0×10^4, 5.0×10^3, 2.5×10^3, 1.0×10^3, 5.0×10^2, 1.0×10^2, 1.0×10^1, 1.0×10^0, and 1.0×10^{-1} Pa, respectively.

During the calculation, we assumed that all energy deposited in the ECU is utilized to produce EHPs, and all generated EHPs are collected to produce electric energy. Therefore, the maximum short-circuit current (I_{sc}) can be expressed as

$$I_{sc} = \frac{qE_{dep}}{E_{ehp}}, \tag{2}$$

where q is the electric charge, E_{dep} refers to the energy of beta particles deposited in the ECU, and E_{ehp} is the average energy required to generate an EHP (the E_{ehp} of silicon is 3.636×10^{-6} MeV). For an ideal PN junction betavoltaic, the open-circuit voltage (V_{oc}) can be expressed as

$$V_{oc} = \frac{kT}{q}\ln\left(\frac{I_{sc}}{I_0}+1\right), \tag{3}$$

where k indicates the Boltzmann constant and I_0 is the reverse saturation current. The minimum value of I_0 can be expressed as [17]

$$I_0 = S\cdot 1.5\times10^5\exp\left(-\frac{E_g}{kT}\right), \tag{4}$$

where S is the PN junction area and E_g is the band gap of silicon.

The maximum output power (P_{max}) is

Table 1 Shape, size, and apparent activity density of ^{63}Ni

Shape	External diameter (mm)	Active diameter (mm)	Apparent activity density for factory (Bq cm^{-2})	Apparent activity density in testing (Bq cm^{-2})
Disc	30	25	7.4×10^7	7.26×10^7
Disc	30	25	1.85×10^8	1.81×10^8

$$P_{max} = I_{sc}V_{oc}\mathrm{FF}, \quad (5)$$

where FF is the fill factor, which can be expressed as

$$\mathrm{FF} = [v_{oc} - \ln(v_{oc} + 0.72)] / (v_{oc} + 1), \quad (6)$$

where n_{oc} is the normalized open-circuit voltage, namely, $V_{oc}/kT/q$.

2.3 Fabrication and measurement

The ECUs for the betavoltaic were manufactured through ion implantation and conventional thermal annealing. B^+ with 50 keV and 1×10^{15} cm^{-2} was implanted in the front of silicon substrate, and P^+ with 60 keV and 2×10^{15} cm^{-2} was implanted in the back of that. To reduce the tunneling effect, a 30 nm thick SiO_2 layer was grown on the front surface of Si via thermal oxidation prior to implantation. After implantation, thermal annealing was performed for 30 min. The active area of the ECU is 0.5 × 0.5 cm^2. The back electrode of each ECU was connected to the printed circuit board pad through conductive silver adhesive, and down-leads were attached to the front electrode of each ECU through gold ball bonding. Insulated brackets were then utilized to fix the ^{63}Ni above the ECU. A 0.7 mm air gap between ^{63}Ni and the ECU was employed in the experiment, as illustrated in Figure 1.

The effect of vacuum degree on the betavoltaic was investigated with low vacuum equipment, as shown in Figure 1. The *I-V* characteristic of the betavoltaic was measured with a Keithley 2636A SourceMeter at 1.0×10^5 and 1.0×10^4 Pa, respectively. Each set of data was tested thrice. The mean value with standard deviation (SD) was recorded. The dark current characteristic was also measured. The values of I_{sc}, V_{oc}, and P_{max} of the betavoltaic can be extracted from the measured *I-V* curves. The short-circuit current, I_{sc}, is the current through the betavoltaic when the voltage across the battery is zero. The open-circuit voltage, V_{oc}, is the maximum voltage available from a betavoltaic and this occurs at zero current. P_{max} is the maximum value of the product of current and voltage. The values of FF is the ratio of P_{max} to the product of I_{sc} and V_{oc}.

3 Results

3.1 Calculation results

The energy deposited in the ECU increases as the vacuum degree increases and reaches the saturation level when the vacuum degree reaches approximately 1.0×10^2 Pa in the calculation (Figure 2). The low apparent activity density ^{63}Ni makes a larger increasing energy deposition rate in the ECU than the high one. For 7.26×10^7 Bq cm^{-2} ^{63}Ni, the value of E_{dep} increases from 2.618×10^5 to 3.055×10^5 MeV, with a 16.68% increase, as the vacuum degree increases from 1.0×10^5 to 1.0×10^{-1} Pa. For 1.81×10^8 Bq cm^{-2} ^{63}Ni, it increases from 7.164×10^5 to 8.132×10^5 MeV, with a 13.52% increase.

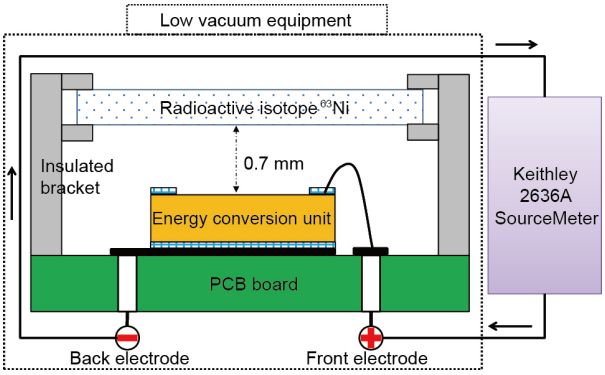

Figure 1 (Corlor online) Measurement schematic of the betavoltaic.

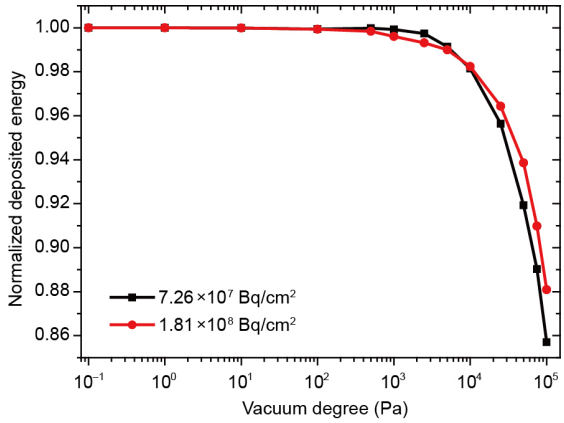

Figure 2 (Corlor online) Normalized energy deposited in the ECU as a function of vacuum degree in the calculation.

As shown in see Figure 3(a) and (b), the output performances of the betavoltaic increase as the vacuum degree increases and reach their saturation values when the vacuum degree reaches approximately 1.0×10^2 Pa in the calculation. The largest change takes place in P_{max}, followed by I_{sc} and V_{oc}, whereas the change in FF is smallest. The improved efficiencies of the betavoltaic performances based on low apparent activity density ^{63}Ni are greater than those based on high apparent activity density ^{63}Ni. Table 2 shows the calculated output performances of the betavoltaics at 1.0×10^5, 1.0×10^4, and 1.0×10^{-1} Pa, respectively. When the vacuum degree increases from 1.0×10^5 to 1.0×10^{-1} Pa, the obtained values of I_{sc}, V_{oc}, P_{max}, and FF increase by 16.68%, 1.06%, 18.19%, and 0.23% for 7.26×10^7 Bq cm^{-2} ^{63}Ni and by 13.52%, 0.82%, 14.64%, and 0.17% for 7.26×10^7 Bq cm^{-2} ^{63}Ni, respectively.

3.2 Measurement results and corresponding calculation results

Figure 4 shows a set of the measured *I-V* characteristics of the betavoltaics. The performance of the betavoltaic improves as the vacuum degree increases. Table 3 shows the output performances of the betavoltaics in the experiment. The mean values with SDs of I_{sc}, V_{oc}, P_{max}, and FF were extracted from

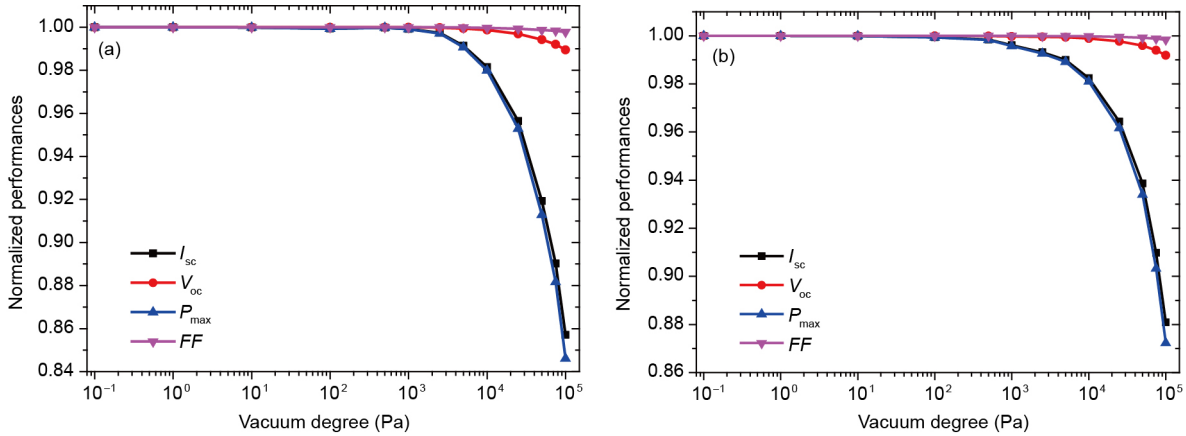

Figure 3 (Corlor online) Normalized I_{sc}, V_{oc}, P_{max}, and FF of the betavoltaic as a function of vacuum degree irradiated by (a) 7.26×10^{7} and (b) 1.81×10^{8} Bq cm^{-2} ^{63}Ni in the calculation.

Table 2 Calculated performances of the betavoltaic at 1.0×10^{5}, 1.0×10^{4} and 1.0×10^{-1} Pa

Activity density (Bq cm^{-2})	Vacuum degree (Pa)	I_{sc} (A)	V_{oc} (V)	P_{max} (W)	FF (%)
7.26×10^{7}	1.0×10^{5}	1.154×10^{-8}	0.3752	3.290×10^{-9}	76.00
	1.0×10^{4}	1.321×10^{-8}	0.3787	3.810×10^{-9}	76.15
	1.0×10^{-1}	1.346×10^{-8}	0.3792	3.888×10^{-9}	76.17
1.81×10^{8}	1.0×10^{5}	3.157×10^{-8}	0.4012	9.762×10^{-9}	78.39
	1.0×10^{4}	3.520×10^{-8}	0.4040	1.098×10^{-8}	77.18
	1.0×10^{-1}	3.583×10^{-8}	0.4045	1.119×10^{-8}	77.20

Table 3 Output performances of the betavoltaics in the measurement (mean ± SD, in %)

Activity density (Bq cm^{-2})	Vacuum degree (Pa)	I_{sc} (A)	V_{oc} (V)	P_{max} (W)	FF (%)
7.26×10^{7}	1.0×10^{5}	2.188×10^{-9} ±0.65	0.0581 ±1.95	4.601×10^{-11} ±4.84	36.2 ±2.32
	1.0×10^{4}	2.637×10^{-9} ±0.34	0.0633 ±0.24	6.195×10^{-11} ±0.77	37.1 ±2.2
1.81×10^{8}	1.0×10^{5}	4.935×10^{-9} ±0.45	0.0747 ±0.23	1.465×10^{-10} ±0.56	39.8 ±0.74
	1.0×10^{4}	5.882×10^{-9} ±0.06	0.0791 ±0.37	1.909×10^{-10} ±0.78	41.0 ±0.77

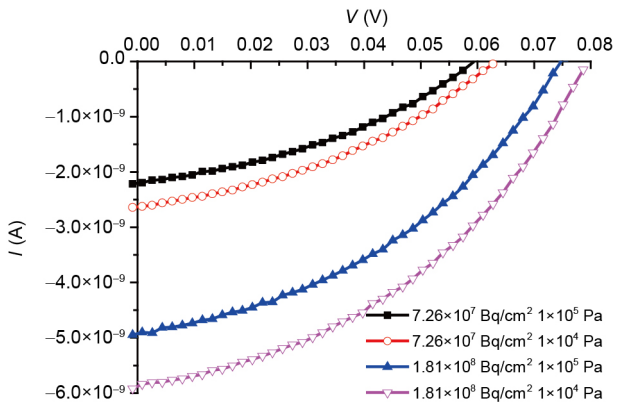

Figure 4 (Corlor online) The measured *I-V* characteristics of the betavoltaics.

three sets of the *I-V* characteristics of the betavoltaics.

According to the data in Tables 2 and 3, the improved efficiencies of I_{sc}, V_{oc}, P_{max}, and FF were obtained as the vacuum degree increases from 1.0×10^{5} to 1.0×10^{4} Pa in both the calculation and measurement (Figure 5). In Figure 5, the terms of 'Cal.' and 'Meas.' means the calculation and measurement values, and the terms of 'low' and 'high' ^{63}Ni means low and high apparent activity density ^{63}Ni, respectively. With the increase of the vacuum degree, the output performances of the betavoltaic in the measurement exhibit the same trends as do those in the calculation. The largest change takes place in P_{max}, followed by I_{sc}, V_{oc}, and FF. Moreover, the high apparent activity density ^{63}Ni makes a smaller improved efficiency on the betavoltaic performances than the low one. However, contrary to the calculated results, the measured FF improved efficiency for the high apparent activity density ^{63}Ni is slightly larger than that for the low one. In addition to this, the improved efficiencies of calculated I_{sc}, V_{oc}, P_{max}, and FF are all smaller than those of the measured ones with low or high apparent activity density ^{63}Ni.

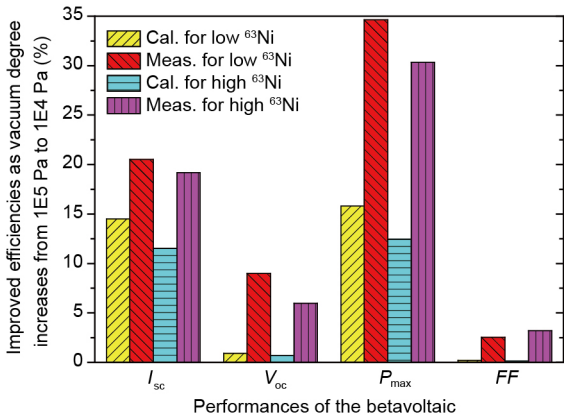

Figure 5 (Corlor online) Modified improved efficiencies of I_{sc}, V_{oc}, P_{max}, and FF as vacuum degree increases from 1.0×10^5 to 1.0×10^4 Pa in the calculation and measurement.

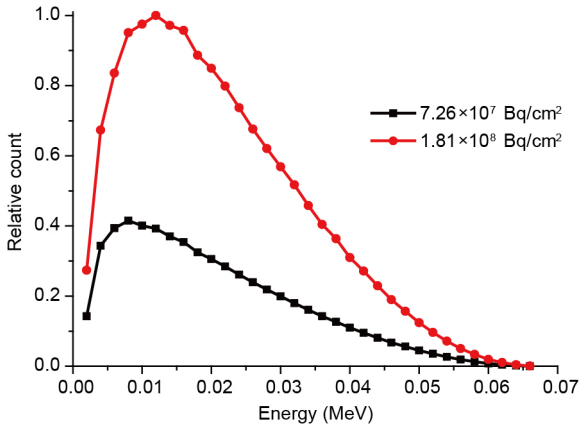

Figure 6 (Corlor online) Apparent emission energy spectra of ^{63}Ni calculated by MCNP5.

4 Discussion

Betavoltaic performance depends mainly on the energy deposition in the ECU. When the vacuum degree is low, the air density in the gap between the source ^{63}Ni and the ECU quickly decreases as the vacuum degree increases. This phenomenon allows more beta particles to traverse the air gap, deposit more energy in the ECU, and consequently improves the betavoltaic performance. When the vacuum degree is high, the gap air becomes so thin that most beta particles can pass through the air gap. Continuing to increase the vacuum degree will barely enhance the energy deposition. Thus, the resulting performance of the betavoltaic is almost changeless.

The increase in energy deposition leads to an increase in the number of generated EHPs and the subsequent I_{sc} value. V_{oc} increases logarithmically with increasing I_{sc}, and so increases gradually as the vacuum degree increases. According to eq. (6), FF increases gradually as V_{oc} increases. According to eq. (5), P_{max} is the product of I_{sc}, V_{oc}, and FF, and so exhibits the largest change.

The vacuum degree dependence of the increasing energy deposition rate is related to the emission energy spectrum of the beta source. The apparent emission energy spectra were obtained theoretically by the surface current tally card to record the beta particles emitted from the source surface in all energy bins with the help of MCNP5. Ref. [18] has studied the influences of ^{63}Ni and ^{147}Pm source thickness on betavoltaics, and found that the shape of the apparent emitted energy spectrum is not fixed with the source thickness changes. Figure 6 shows that when the apparent activity density of ^{63}Ni increases from 7.26×10^7 to 1.81×10^8 Bq cm^{-2}, the peak of the energy spectra moves toward the high energy section because of the self-absorption effect. This similar behavior was demonstrated by ^{147}Pm [18], ^{90}Sr-^{90}Y [19], and ^{3}H [20]. Compared with low apparent activity density ^{63}Ni, the high one allows beta particles to traverse the air gap into the ECU more easily. The number of beta particles stopped or absorbed by the air gap for low apparent activity density ^{63}Ni decreases considerably when the vacuum degree increases. Therefore, the energy deposition for low apparent activity density ^{63}Ni increases more rapidly than that for the high one. The same phenomenon was exhibited in the output performances of the betavoltaic.

Low apparent activity density results in low I_{sc} and a low ratio of I_{sc}/I_0, which leads to a high sensitivity of V_{oc} [3,13]. Accordingly, the vacuum degree effect on the P_{max} of the betavoltaic with low apparent activity density ^{63}Ni is more significant than that of the betavoltaic with the high one.

The minimum reverse saturation current was employed during the calculation. However, in practice, non-ideal surface treatment, such as passivation, can result in a low I_0 value and a low ratio of I_{sc}/I_0. Shunt resistance (R_{sh}) usually reflects the degree of leakage current through the device, and the ideality factor (n) refers to the recombination mechanisms of majority and minority carriers. As shown in Figure 5, it is revealed that there are large gaps between the calculation results and the measurement ones. Therefore, the previous calculation process should be modified with these three terms, including I_0, n, and R_{sh}, to reduce those gaps. The values of I_0, R_{sh}, and n can be extracted from the measured dark current characteristic and the I-V curves irradiated by ^{63}Ni.

The values of I_0 and n were estimated from the relationship between the logarithm of the measured dark current (I_d) and the forward bias voltage. The formula can be express as

$$\ln(I_d) = \frac{q}{nkT}V + \ln(I_0). \tag{7}$$

The intercept of the curve on the Y-axis gives the value of I_0. The slope of the $\ln(I_d)$ versus V is equal to (q/nkT) and gives the value of n. As shown in Figure 7, the values of I_0 and n for the betavoltaic are I_0=2.8×10^{-10} A and n=1.17.

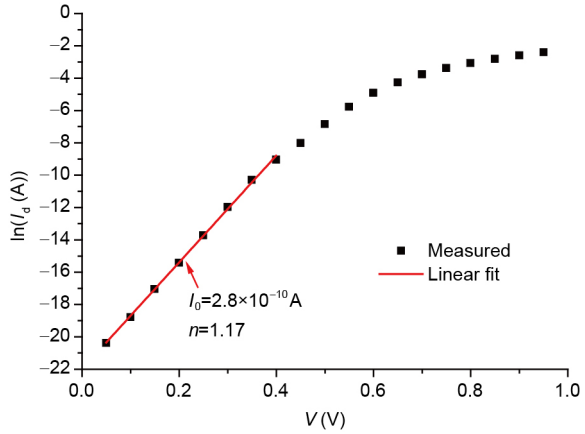

Figure 7 (Corlor online) Dark current characteristic of the betavoltaic.

The R_{sh} value was estimated from the slope of the measured I-V curve irradiated by ^{63}Ni at V=0. The value is expressed as

$$R_{sh} = \left.\frac{dV}{dI}\right|_{V=0, I=I_{sc}}. \quad (8)$$

Table 4 shows the mean values of R_{sh} with SDs. The modified equivalent circuit model can be expressed as

$$I = -I_R + I_0\left\{\exp\left(\frac{qV}{nkT}\right) - 1\right\} + \frac{V}{R_{sh}}, \quad (9)$$

where I_R is radiation-generated current, which is approximately equal to I_{sc} calculated by eq. (2). The I_{sc}, V_{oc}, P_{max}, and FF values of the betavoltaic were calculated with eq. (9).

The values of I_0, n, and R_{sh} extracted from the measurement results were estimated to modify the equivalent circuit model. The modified model was used to modify the previous calculation results. After that, the modified improved efficiencies of I_{sc}, V_{oc}, P_{max}, and FF as vacuum degree increases from 1.0×10^5 to 1.0×10^4 Pa in the calculation for low and high apparent activity density ^{63}Ni respectively are obtained in Figure 8. The terms of 100% and 50% refer to the collection rate of EHPs in Figure 8. With an EHP collection rate of 100%, the modified calculation improved efficiencies are close to the measurement ones (Figures 5 and 8). However, gaps still exist between the calculated and measured efficiencies. Two reasons may cause this result. First, the beta source ^{63}Ni could fall off naturally during use or storage and make the actual activity density lower than the estimated value by only a half-life. Hence, the apparent activity density should be accurately calibrated prior to measurement. Second, the actual collection rate of the EHPs is lower than the theoretical value. A low collection rate results in low measured I_{sc}, and consequently, a low ratio of I_{sc}/I_0. The modified improved efficiencies of V_{oc}, P_{max}, and FF increase when the collection rate decreases from 100% to 50%. The modified calculation values are closer to the measurement ones. However, the improved efficiency of I_{sc} remains almost the same and still has a large gap with the measurement value because of the influence of series resistance (R_s). A high R_s results in a low I_{sc}. Moreover, the value of R_s decreases with the intensity of illumination [21], which is equivalent to the activity density of the incident beta particles. A low vacuum degree results in high R_s and small I_{sc}. By contrast, a high vacuum degree results in low R_s and large I_{sc}. However, the effects of R_s on I_{sc} and other aspects of betavoltaic performance require further study.

To enhance the vacuum degree resistance in applications, the betavoltaic should employ high apparent activity density sources, high-quality semiconductor materials, and optimized micro-nano processing technology. Vacuum packaging could also be introduced to the betavoltaic with a recommended value of 1.0×10^2 Pa.

5 Conclusions

We presented a theoretical method to study the vacuum degree effects on betavoltaics based on ^{63}Ni with different

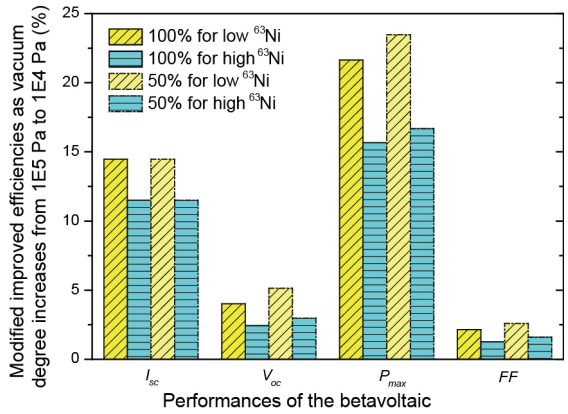

Figure 8 (Corlor online) Modified improved efficiencies of I_{sc}, V_{oc}, P_{max}, and FF as vacuum degree increases from 1.0×10^5 to 1.0×10^4 Pa in the calculation based on 100% and 50% EHPs collection rate respectively.

Table 4 R_{sh} Values of the betavoltaic (mean ± SD, in %)

Activity density (Bq cm^{-2})	Vacuum degree (Pa)	R_{sh} (Ω)
7.26×10^7	1.0×10^5	7.45×10^7±5.32
	1.0×10^4	7.45×10^7±0.57
1.81×10^8	1.0×10^5	5.78×10^7±2.20
	1.0×10^4	5.71×10^7±1.15

apparent activity densities. The *I-V* characteristics of betavoltaics were measured at 1.0×10^5 and 1.0×10^4 Pa and compared with those in the calculation results. The results show that the betavoltaic performances improve significantly as the vacuum degree increases. The largest change is in P_{max}, followed by I_{sc}, V_{oc}, and FF. The vacuum degree effect on the energy deposition for low apparent activity density ^{63}Ni is more significant than that for the high one. The same result was obtained for the improved efficiencies of I_{sc}, V_{oc}, and P_{max} of the betavoltaic. Furthermore, the improved efficiencies of the performances, including I_{sc}, V_{oc}, P_{max}, and FF, in the measurement are higher than those in the calculation because of the low rate of I_{sc}/I_0. I_0, n, and R_{sh} were estimated to modify the equivalent circuit model. The calculation results based on this model are closer to the measurement results. This research can serve as a reference to study the vacuum degree effects on betavoltaics based on other semiconductor materials and beta sources.

This work was supported by the National Natural Science Foundation of China (Grant Nos. 11505096 & 11675076), the National Defense Basic Scientific Research Project (Grant No. JCKY2016605C006), the Natural Science Foundation of Jiangsu Province (Grant No. BK20150735), the Shanghai Aerospace Science and Technology Innovation Fund, the Jiangsu Planned Projects for Postdoctoral Research Funds (Grant No. 1601139B), the Foundation of Graduate Innovation Center in NUAA (Grant No. kfjj20160609), the Priority Academic Program Development of Jiangsu Higher Education Institutions, and the Fundamental Research Funds for the Central Universities (Grant No. NJ20160031).

1 Luo S Z, Wang G Q, Zhang H M. Advance in radiation-voltaic isotope battery. J Isot, 2011, 24: 3–13
2 Ghasemi Nejad G R, Rahmani F, Abaeiani G R. Design and optimization of beta-cell temperature sensor based on ^{63}Ni–Si. Appl Radiat Isot, 2014, 86: 46–51
3 Liu Y P, Tang X B, Xu Z H, et al. Optimization and temperature effects on sandwich betavoltaic microbattery. Sci China Tech Sci, 2014, 57: 14–18
4 Wang H, Tang X, Liu Y P, et al. Temperature effect on betavoltaic microbatteries based on Si and GaAs under ^{63}Ni and ^{147}Pm irradiation. Nucl Instruments Methods Phys Res Sect B-Beam Interactions Mater Atoms, 2015, 359: 36–43
5 Chen H, Jiang L, Chen X. Design optimization of GaAs betavoltaic batteries. J Phys D-Appl Phys, 2011, 44: 215303
6 Li F H, Gao X, Yuan Y L, et al. GaN PIN betavoltaic nuclear batteries. Sci China Tech Sci, 2014, 57: 25–28
7 San H, Yao S, Wang X, et al. Design and simulation of GaN based Schottky betavoltaic nuclear micro-battery. Appl Radiat Isot, 2013, 80: 17–22
8 Munson Iv C E, Arif M, Streque J, et al. Model of Ni-63 battery with realistic PIN structure. J Appl Phys, 2015, 118: 105101
9 Qiao D Y, Chen X J, Ren Y, et al. A micro nuclear battery based on SiC schottky barrier diode. J Microelectromech Syst, 2011, 20: 685–690
10 Gui G, Zhang K, Blanchard J P, et al. Prediction of 4H–SiC betavoltaic microbattery characteristics based on practical Ni-63 sources. Appl Radiat Isot, 2016, 107: 272–277
11 Qiao D Y, Yuan W Z, Gao P, et al. Demonstration of a 4H SiC betavoltaic nuclear battery based on schottky barrier diode. Chin Phys Lett, 2008, 25: 3798–3800
12 Lei Y, Yang Y, Liu Y, et al. The radiation damage of crystalline silicon PN diode in tritium beta-voltaic battery. Appl Radiat Isot, 2014, 90: 165–169
13 Liu Y, Tang X, Xu Z, et al. Experimental and theoretical investigation of temperature effects on an interbedded betavoltaic employing epitaxial Si and bidirectional ^{63}Ni. Appl Radiat Isot, 2014, 94: 152–157
14 Lu M, Zhang G, Fu K, et al. Gallium Nitride Schottky betavoltaic nuclear batteries. Energ Conv Manage, 2011, 52: 1955–1958
15 Wacharasindhu T, Nullmeyer B R, Kwon J W, et al. Mechanisms leading to losses in conventional betavoltaics and evolution: Utilizing composite semiconductor with infused radioisotope for efficiency improvement. J Microelectromech Syst, 2014, 23: 56–65
16 Bao R, Brand P J, Chrisey D B. Betavoltaic performance of radiation-hardened high-efficiency Si space solar cells. IEEE Trans Electron Devices, 2012, 59: 1286–1294
17 Martin A G. Solar Cells: Operating Principles, Technology and System Applications. Englewood Cliffs: Prentice-Hall, 2012
18 Liu Y, Tang X, Xu Z, et al. Influences of planar source thickness on betavoltaics with different semiconductors. J Radioanal Nucl Chem, 2015, 304: 517–525
19 Rappaport P, Loferski J J, Linder E G. The electron-voltaic effect in germanium and silicon p-n junctions. RCA Rev, 1956, 17: 100–134
20 Li H, Liu Y, Hu R, et al. Simulations about self-absorption of tritium in titanium tritide and the energy deposition in a silicon Schottky barrier diode. Appl Radiat Isot, 2012, 70: 2559–2563
21 Priyanka , Lal M, Singh S N. A new method of determination of series and shunt resistances of silicon solar cells. Sol Energ Mater Sol Cells, 2007, 91: 137–142